Distributions of the S-matrix poles in Woods-Saxon and cut-off Woods-Saxon potentials

P. Salamon[a], Á. Baran[b], T. Vertse[a,b,*]

[a] *MTA Institute for Nuclear Research, Debrecen, PO Box 51, H–4001, Hungary*
[b] *Faculty of Informatics, University of Debrecen, PO Box 400, H–4002 Debrecen, Hungary*

arXiv:1511.06565v3 [nucl-th] 19 Apr 2016

Abstract

The positions of the $l = 0$ S-matrix poles are calculated in generalized Woods-Saxon (GWS) potential and in cut-off generalized Woods-Saxon (CGWS) potential. The solutions of the radial equations are calculated numerically for the CGWS potential and analytically for GWS using the formalism of Gy. Bencze [1]. We calculate CGWS and GWS cases at small non-zero values of the diffuseness in order to approach the square well potential and to be able to separate effects of the radius parameter and the cut-off radius parameter. In the case of the GWS potential the wave functions are reflected at the nuclear radius therefore the distances of the resonant poles depend on the radius parameter of the potential. In CGWS potential the wave function can be reflected at larger distance where the potential is cut to zero and the derivative of the potential does not exist. The positions of most of the resonant poles do depend strongly on the cut-off radius of the potential, which is an unphysical parameter. Only the positions of the few narrow resonances in potentials with barrier are not sensitive to the cut-off distance. For the broad resonances the effect of the cut-off can not be corrected by using a suggested analytical form of the first order perturbation correction.

Keywords: S-matrix, Woods-Saxon potential, potentials

1. Introduction

Exactly solvable quantum mechanical models proved to be invaluable tools in the understanding of many fundamental quantum mechanical concepts. In particular, they give insight into complex phenomena, like the symmetries of quantum mechanical systems, and they also allow the investigation of transitions through critical parameter domains [2]. Our goal in this paper is more simple, and analytical solution serves as a firm basis of numerical integration of the radial Schroedinger equation.

*Corresponding author
Tel.: +3652509231; *fax:* +3652416181
E-mail address: vertse.tamas@atomki.mta.hu

In this work we consider a very simple case in which a neutral particle is scattered on a spherically symmetric target nucleus represented by a real Woods-Saxon (WS) type [3] nuclear potential $v(r)$. The WS potential is the most common phenomenological nuclear potential used in the description of nuclear reactions in the Gamow shell model (GSM) description [4] of drip line nuclei. A recent analysis of this type is the description of the ^{7}Be(p,γ)^{8}B and the ^{7}Li(n,γ)^{8}Li reactions in Ref. [5]. The key elements of GSM are the Berggren-ensembles of single particle states. The Berggren-ensemble might include resonant and sometime anti-bound states beside the bound states and the scattering states along a complex path. The shape of the path determines the set of the S-matrix pole states to be included in the ensemble. In order to have smooth contribution from the scattering states the shape of the path should go reasonably far from the poles. Therefore to know, where the poles are located has crucial importance.

The WS potential was introduced long time ago as a smoothed replacement of the square well (SQ) potential, because the sudden jump of the constant depth of the potential to zero was considered unrealistic in the SQ potential. An introduction of a diffuseness parameter simulated the gradual decrease of the potential value in the surface region of the nucleus. The only disadvantage of the diffuse potential was that the closed analytical form of the solution of the radial Schroedinger equation had to be sacrificed. More precisely, for zero angular momentum the solution could be calculated analytically but for higher partial waves the equation could be solved without approximation [6] only by using numerical integration. In this work we use the opportunity of having both analytic and numeric solutions for the $l = 0$ case and compare the distribution of the poles of the scattering matrix S for the two types of the potentials.

In section 2 of the paper we define the poles of the S-matrix on the complex k-plane for zero angular momentum. In section 3 we give analytical formulae of the S-matrix for WS and GWS potentials. In section 4 and 5 we present the cut-off versions of the potentials (CWS and CGWS potentials) and the numerical methods for calculating the positions of the resonant poles and the normalization of the resonant wave functions. A simple perturbation correction of the cut-off of these potentials is also given in the section 5. Section 6 contains the results of the numerical examples for heavy and light nuclear systems. The summary of the results is given in section 7.

2. Poles of the S-matrix on the complex k plane

The nuclear potential $v(r)$ determines the so called *squared local wave number*

$$k^2(r) = [k^2 - v(r)] \ , \tag{1}$$

and the radial Schroedinger equation to be solved is

$$u''(r,k) + k^2(r)u(r,k) = 0 \ . \tag{2}$$

Here prime denotes the derivative with respect to (wrt) the radial distance r.

The first boundary condition (BC) for the solution $u(r,k)$ is its regularity at $r=0$:

$$u(0,k)=0\ . \tag{3}$$

The other BC is specified in the asymptotic region, where the nuclear potential becomes zero, and the solution $u(r,k)$ is proportional to a combination of the incoming e^{-ikr} and outgoing e^{ikr} free spherical waves:

$$u(r,k)=C[e^{-ikr}-S_{l=0}(k)e^{ikr}]\ . \tag{4}$$

The ratio of the two type of solutions is fixed by the element of the scattering matrix $S_0(k)$. For scattering solutions the BC in Eqs. (3) and (4) can be satisfied for any value of k.

For the poles of $S(k)$ the BC should be of purely outgoing type. For a decaying resonance the solution in the asymptotic region is proportional to e^{ikr}. The poles of $S_0(k)$ for a real potential are either real energy poles (bound and anti-bound poles) or complex energy poles. The real energy poles lie on the imaginary k-axis. The complex energy poles are the resonances. The decaying resonances lie in the fourth quadrant of the k plane. The mirror images of the decaying resonances are the capturing resonances in the third quadrant. The complex wave number of a decaying (Gamow or Gamow-Siegert) resonance is denoted by $k=k^R+ik^I$ with $k^I<0$, and $k^R>0$, and by $k^R<0$ for a capturing resonance. Since the energy is proportional to k^2, therefore the unbound poles (i.e. the anti-bound poles and the resonances) lie on the second energy-sheet.

3. WS and GWS potentials

We want to study the dependence of the resonant pole positions on the tail of the nuclear potential. We compare the pole structure of the potentials without any cut and that of the cut-off potentials. A SQ potential is zero beyond its radius but the WS potential becomes zero only at infinity. It is convenient to write the WS potential as a product of its strength V_1

$$V^{WS}(r)=V_1 f^{WS}(r)\ , \tag{5}$$

and its radial shape:

$$f^{WS}(r)=-\frac{1}{1+e^{\frac{r-R}{a}}}\ . \tag{6}$$

This shape has two parameters, the radius R and the diffuseness a. The exponential tail in Eq. (5) tends to zero when the radial distance r goes to infinity. To calculate scattering cross-sections we need the matrix element of the scattering matrix S. The value of S_0 can be calculated from matching the solution of the radial Schroedinger equation to that of the asymptotical solution. For a WS potential the matching to the asymptotic solutions can be done only at infinite distance. Sometimes we can complement the WS potential with a surface type term with radial shape

$$f^{SWS}(r)=-\frac{e^{\frac{r-R}{a}}}{(1+e^{\frac{r-R}{a}})^2}\ , \tag{7}$$

and strength V_2 and consider the so called generalized WS potential (GWS)

$$V^{GWS}(r) = V_1 f^{WS}(r) + V_2 f^{SWS}(r) \ . \tag{8}$$

For $l = 0$ the solution is given analytically by Gy. Bencze [1] and very recently by O. Bayrak and E. Aciksoz [7]. Thanks to the analytical solution the matching to the free solution can be performed at infinity. For GWS potential the $l = 0$ scattering matrix element $S_0(k)$ at the complex wave number k is given in Ref. [1] as follows:

$$S_0(k) = \exp(-2ikR)\frac{\Gamma(2ika)}{\Gamma(-2ika)} \cdot \frac{A\frac{\Gamma(1-2\lambda)}{\Gamma(1-\lambda-\mu+ika)\Gamma(-\lambda+\mu+ika)} - \frac{\Gamma(1+2\lambda)}{\Gamma(\lambda+\mu+ika)\Gamma(1+\lambda-\mu+ika)}}{\frac{\Gamma(1+2\lambda)}{\Gamma(1+\lambda-\mu-ika)\Gamma(\lambda+\mu-ika)} - A\frac{\Gamma(1-2\lambda)}{\Gamma(-\lambda+\mu-ika)\Gamma(1-\lambda-\mu-ika)}} \ , \tag{9}$$

where $\Gamma(z)$ stands for the Gamma function with complex argument z, see e.g. [8].

$$A = \Big(\frac{b}{1+b}\Big)^{2\lambda}(1+b)^{-2ika}\frac{{}_2F_1(\lambda+\mu+ika, 1+\lambda-\mu+ika, 1+2\lambda; \frac{b}{1+b})}{{}_2F_1(-\lambda+\mu-ika, 1-\lambda-\mu-ika, 1-2\lambda; \frac{b}{1+b})} \ , \tag{10}$$

where $b = e^{-R/a}$ and ${}_2F_1(a, b, c; z)$ stands for the Hyper-geometric Function [8] with complex argument z. The parameters have the following values:

$$\lambda = ika\sqrt{1+\frac{V_1}{E}} \ , \mu = \frac{1}{2} + \frac{1}{2}\sqrt{1+4k^2a^2\frac{V_2}{E}} \ , \text{and } E = \frac{\hbar^2k^2}{2M} \ . \tag{11}$$

The complex energy E is calculated from the complex wave number k by using the reduced mass M of the target nucleus plus neutron system. In order to find the poles of $S_0(k)$ in a domain of the complex k-plane we search for the zeros of $D(k)$, which is the denominator in Eq. (9):

$$D(k) = \frac{\Gamma(1+2\lambda)}{\Gamma(1+\lambda-\mu-ika)\Gamma(\lambda+\mu-ika)} - A\frac{\Gamma(1-2\lambda)}{\Gamma(-\lambda+\mu-ika)\Gamma(1-\lambda-\mu-ika)} \ . \tag{12}$$

The zero of $D(k)$ is found by the program BENCZE written in Wolfram Mathematica. Having the discrete set of zeros k_m in the fourth k-quadrant

$$D(k_m) = 0 \ , \tag{13}$$

we can order them as the $k^R > 0$ values increase. The bound and the anti-bound poles along the imaginary k-axis are ordered differently, according to the number of the nodes n in the radial wave function excluding the origin.

The $a \to 0$ limit of the WS potential in Eq. (5) corresponds to the SQ potential. Poles in the square well potential were studied extensively by Nussenzveig [9]. He showed, that for $l = 0$ the pole trajectories converge to asymptotes with $k_m^R = \frac{m\pi}{R}$ as the depth $V_1 \to 0$. The distance of the consecutive poles is determined basically by the radius of the square

well R, where the wave function is reflected. For large m values the distance between two consecutive resonant poles: $|k_{m+1} - k_m|$ approaches the value of $\frac{\pi}{R}$, so we can approximate the m dependence of the pole position k_m for large m by

$$k_m^R = \frac{m\pi}{R} + O(1) \ . \tag{14}$$

In the book of R. Newton [10] a similar expression is given for the real parts of the starting values of the k-trajectories. The values there were given for so called strictly finite range (SFR) potentials vanishing at and beyond R_{max} [11]. For a SQ potential the radius R and the finite range R_{max} is the same distance. The WS or the GWS potentials become zero only at infinite distance, therefore they are not SFR type potentials. In Ref. [12] it was shown that for some types of the SFR potentials the starting points of the pole trajectories (staring point of a trajectory is a k value belonging to very small potential strength V_1) can be described by a relation:

$$|k_m| = \frac{m\pi}{R} + O(1) \ . \tag{15}$$

Although these findings was observed for very small V_1 values, we speculate that Eq. (15) might be valid approximately for realistic values of V_1, too. Therefore after calculating the complex k_m eigenvalues with realistic values of V_1 we tried to fit the $|k_m|$ values by a first order polynomial:

$$p(m) = a_0 + a_1 m \ . \tag{16}$$

The best fit first order polynomial minimizes the sum of the squares of the differences:

$$\Delta(a_0, a_1) = \sum_{m=m_s}^{m_u} [|k_m| - p(m)]^2 \to \min \ . \tag{17}$$

From the slope a_1 of the best fit polynomial we can deduce a distance $\mathcal{R}$ based on the relation:

$$\mathcal{R} = \frac{\pi}{a_1} \ . \tag{18}$$

Since the relation in Eq. (15) expected to be valid for large m values, we apply a lower cut m_s for the m values and check the validity of the linear behavior as m_s increases. The upper value of the index m_u is fixed at a large value.

4. Cut-off WS and GWS potentials

By cutting off the WS potential or the GWS potential to zero at a finite R_{max} distance we can convert them to SFR potential and solve the radial equation by numerical integration.

At the direct numerical integration we proceed from the origin $r = 0$ step by step to R_{max} where the nuclear potential becomes zero. At or beyond this distance, i.e. at $R_a \geq R_{max}$ we match the numerical solution to that of the free solution and calculate $S_0(k)$. The cut-off Woods-Saxon potential (CWS) has the form:

$$V^{CWS}(r) = V_1 f^{CWS}(r) \ , \tag{19}$$

where the radial shape is

$$f^{CWS}(r) = -\begin{cases} \frac{1}{1+e^{\frac{r-R}{a}}} & , \text{if } r < R_{max} \\ 0 & , \text{if } r \geq R_{max} \ . \end{cases} \tag{20}$$

In the cut-off GWS (CGWS) form the surface potential term in Eq. (7) is cut to zero at the same R_{max} distance.

Although the method of the numerical calculation of the k_m eigenvalues are given in several places, see e.g. Refs. [13],[14], [15], let us sketch briefly how the pole solutions of the radial equation are calculated numerically. We introduce left and right solutions of the radial equation in Eq. (2) and an intermediate distance R_{id}, which separates the left and right regions. A left solution satisfies the initial values:

$$u_{left}(0,k) = 0, \text{ and} \qquad u'_{left}(0,k) = 1 \ , \tag{21}$$

and it is defined in the $r \in [0, R_{id}]$ interval. We get it by integrating the Eq. (2) numerically from the origin until R_{id}, where we calculate the logarithmic derivative of the left solution:

$$L_{left}(k, R_{id}) = \frac{u'_{left}(R_{id},k)}{u_{left}(R_{id},k)} \ . \tag{22}$$

The right solution satisfies outgoing boundary condition at the distance $R_a \geq R_{max}$, where the nuclear potential is zero, therefore the initial values for the right solution are outgoing waves:

$$u_{right}(R_a,k) = e^{ikR_a}, \text{ and} \qquad u'_{right}(R_a,k) = ike^{ikR_a} \ . \tag{23}$$

The right solution is defined in the $r \in [R_{id}, R_a]$ interval. We integrate radial equation in Eq. (2) numerically in backward direction, starting from R_a till $r = R_{id}$, where we calculate the logarithmic derivative of the right solution:

$$L_{right}(k, R_{id}) = \frac{u'_{right}(R_{id},k)}{u_{right}(R_{id},k)} \ . \tag{24}$$

The eigenvalue k_m of the pole state belongs to the zero of the difference of the left and right logarithmic derivatives:

$$G(k_m, R_{id}) = L_{left}(k_m, R_{id}) - L_{right}(k_m, R_{id}) = 0 \ . \tag{25}$$

The computer programs GAMOW [13], and ANTI [14] find the zeros of $G(k_m, R_{id})$, at certain R_{id} matching distance $0 < R_{id} < R_{max} \leq R_a$. The computer program GAMOW [13] uses Fox-Goodwin method with fix mesh size, and the program ANTI [14] uses the more powerful Ixaru's method [16] for the numerical integration. For a broad resonance the proper choice of the R_{id} matching distance is difficult. The zero is searched by Newton iterations, and the iteration process often converges poorly or fails. Therefore we developed a new method in which we compare the logarithmic derivatives not at a fixed R_{id} distance

but in a wide region in r. This method is built into the program JOZSO[1] [17]. We calculate $G(k_m, r)$ in Eq. (25) at equidistant mesh-points with mesh size h at $r_j = jh$, $j \in [i_1, i_2]$. The mesh points are taken from a region where the nuclear potential falls most rapidly. Then we search for the absolute minimum of the function of two real variables k^R, and k^I:

$$F(k^R, k^I) = \log[\sum_{j=i_1}^{i_2} |G(k, r_j)|] \ . \tag{26}$$

Absolute minima of the function $F(k^R, k^I)$ in Eq. (26) should have a large negative value. The position of the absolute minimum is the pole position of $S(k)$. The minimum of the function is found by using the Powell's method in Ref. [18]. The function $-F(k)$ shows peaks at the minima of $F(k)$. To find the minima of the function $F(k^R, k^I)$ first we explore the landscape of the function $F(k)$ in a complex k domain of our interest. Then we search for the minima of the function $F(k^R, k^I)$ in Eq. (26).

5. Normalized resonant solution

At the pole k_m the left and the right solutions can be matched smoothly, because their logarithmic derivatives are equal, or we take the left solution $u_{left}(r, k_m)$ in the interval $r \in [0, R_a]$ as a non-normalized solution of the radial equation in Eq. (2). Sometimes we need the normalized solution, e.g. in Berggren-ensemble [19] in which all pole solutions are normalized to unity. The square of the norm is composed from the sum of the contributions of the internal and external regions:

$$N^2 = N_{int}^2 + N_{ext}^2 \ . \tag{27}$$

The first one we calculate numerically, by quadrature

$$N_{int}^2 = \int_0^{R_a} u_{left}^2(r) dr \ , \tag{28}$$

while the second one is given analytically as in Ref. [20].

$$N_{ext}^2 = -\frac{u_{left}(R_a, k_m)^2}{2ik_m} \ . \tag{29}$$

Then the normalized solution is simply:

$$u(r, k_m) = \frac{1}{N} u_{left}(r, k_m) \ . \tag{30}$$

[1]The program name is chosen to honor the late József Zimányi to whom one of the authors (T. Vertse) is grateful for starting his carrier.

Using the normalized solution we can estimate the energy shift $\Delta\epsilon_m$ of the pole energy E of the CGWS potential due to the change of the potential without cut. The tail of the resonant normalized solution beyond R_a is an outgoing wave given as

$$Ae^{ik_m r} = \frac{u(R_a, k_m)}{e^{ik_m R_a}} e^{ik_m r} \ . \tag{31}$$

We can try to correct the effect of the cut-off of the tail of the GWS potential on the energy of the resonance using first order perturbation approach as:

$$\Delta\epsilon_m = \int_{R_{max}}^{\infty} V^{GWS}(r) u^2(r, k_m) dr \ , \tag{32}$$

and compare it to the energy difference

$$E(\text{BENCZE}) - E(\text{JOZSO}) \ . \tag{33}$$

If in the volume and in the surface terms of $V^{GWS}(r)$ in Eq. (8) we approximate the fall of the tails of the potentials by $e^{\frac{R-r}{a}}$ in the integration region of Eq. (32), we can approximate the energy difference by the analytic expression

$$\Delta\epsilon_m = \frac{a(V_1 + V_2)A^2}{(1 - 2ik_m a)} \ e^{\frac{R-R_{max}}{a} + 2ik_m R_{max}} \ . \tag{34}$$

A correction for the wavenumber shift Δk_m can be calculated from the energy shift $\Delta\epsilon_m$ by solving a second order algebraic equation

$$\Delta k_m = k_m + \sqrt{k_m^2 + c_1 \Delta\epsilon_m} \ , \tag{35}$$

where c_1 denotes the factor between k^2 in fm^{-2} and the energy E in MeV ($k^2 = c_1 E$). The corrected resonance energy can be written as

$$E_m^{corr} = E_m + \Delta\epsilon_m \ , \tag{36}$$

while the corrected wavenumber of the resonance has the form

$$k_m^{corr} = k_m + \Delta k_m \ . \tag{37}$$

The accuracies of these corrections are checked by comparing the corrected wave numbers to the values calculated by the program BENCZE, see Table 1 of the next chapter.

If the perturbative correction worked well for all poles for $l = 0$ then we could use it later for $l > 0$ when we are unable to handle the problem analytically.

6. Numerical examples

We applied our formalism for two systems in which neutrons are scattered on a heavy target nucleus and on a lighter nucleus. For the first one we choose the ^{208}Pb+n system, with potential parameters $V_1 = 44.4$ MeV, $V_2 = 0$, $r_0 = 1.27$ fm, $a = 0.7$ fm. The radius of the potential is $R = r_0\ 208^{1/3} \approx 7.52$ fm.

For the second example we considered a lighter system studied in Ref. [7]. In that work only bound states ^{56}Fe+n system were calculated, here we extend the studies for resonances.

6.1. WS results for a heavy system

In Fig. 1 we show the $|S_0(k)|$ on the domain $k^R \in [-0.1, 5]$ fm^{-1} and $k^I \in [-4, -0.1]$ fm^{-1} calculated for the WS potential with the parameters listed above. It can be seen

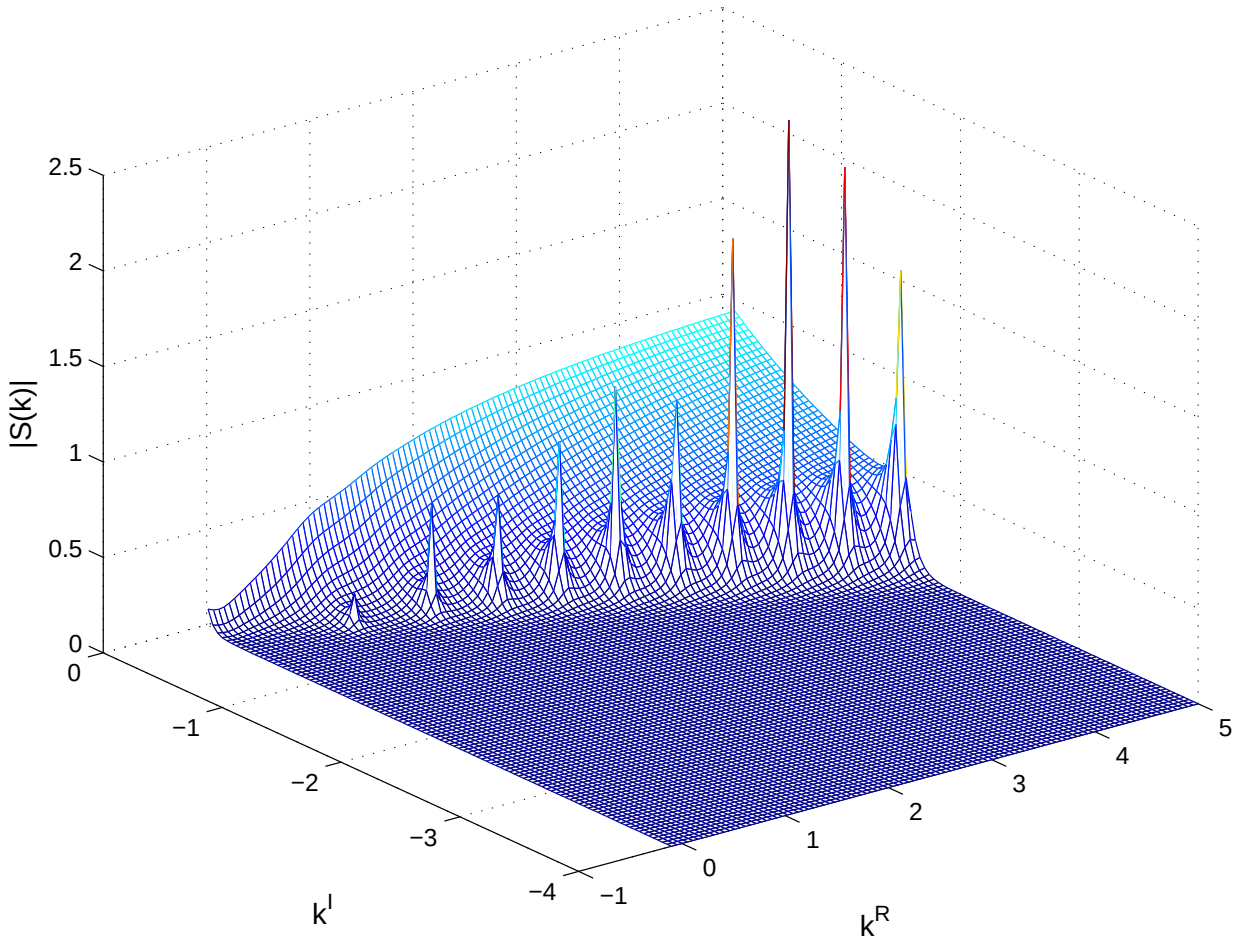

Figure 1: $|S(k)|$ on the domain $k^R \in [-0.1, 5]$ fm^{-1} and $k^I \in [-4, -0.1]$ fm^{-1} calculated for a WS potential with depth parameter: $V_1 = 44.4$ MeV, $V_2 = 0$ MeV, $a = 0.7$ fm, $R = 7.52$ fm

that the poles form a mountain with peaks being almost equidistant in k^R. If we assign a sequence number m to each peaks we can fit a first order polynomial in Eq. (16) to either the k_m^R values as function of m, or to the $|k_m|$ values. We observed that the fits to the k_m^R values and to the $|k_m|$ values produce very similar results. Therefore in the remaining part of this paper we use only the fits to the $|k_m|$ values.

In Fig. 3 we show the a dependence of the slope of the first order polynomial fitted to the $|k_m|$ values calculated for the WS potential with two different values of the diffuseness. The very small, $a = 0.05$ fm value simulates the SQ potential. The other case with $a = 0.7$ fm is the normal diffuseness value for ^{208}Pb.

The horizontal blue line corresponds to the value $\frac{\pi}{R}$, where R is the common radius of the square well and the WS potential. The distance of the asymptotes of the poles in the

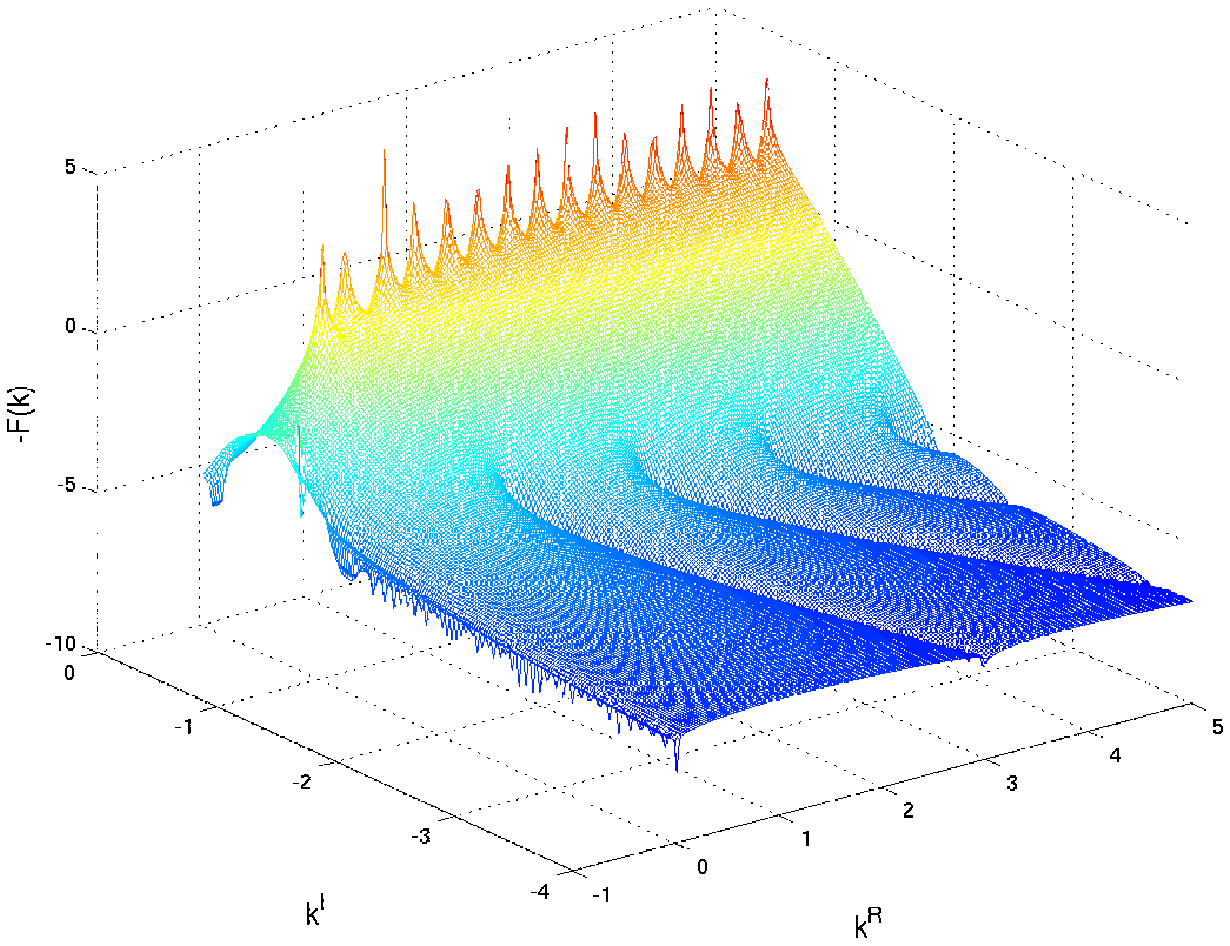

Figure 2: $-F(k)$ on the domain $k^R \in [-0.1, 5]$ fm^{-1} and $k^I \in [-4, -0.1]$ fm^{-1} calculated for a CWS potential with depth parameter: $V_1 = 44.4$ MeV, $V_2 = 0$ MeV, $a = 0.7$ fm, $R = 7.52$ fm, $R_{max} = 12$ fm.

SQ well is $\frac{\pi}{R}$. As m_s increases the a_1 slope values become soon independent on m_s and their values are close to the $\frac{\pi}{R}$ value. This simple property seems to be inherited from the SQ potential to the WS potential. The deviations from this simple rule increase as the value of the diffuseness parameter increases, but the deviations remain within 5% of the $\frac{\pi}{R}$ value for $m_s > 20$ even for $a = 0.7$ fm (red squares). Therefore the estimated range in Eq. (18) is close to the radius parameter of the WS potential.

6.2. CWS results for a heavy system

To compare to the cut-off potentials, we can calculate the positions of the poles in a CWS potential with the same parameters as the WS potential used, but with a cut-off radius $R_{max} = 12$ fm. The distributions of the complex poles can be visualized if we plot the landscape of the function $-F(k)$ defined in Ref. [15] on the same domain of the complex k-plane as we considered in Fig. 1. The results are displayed in Fig. 2.

The peaks of the function $-F(k)$ are at the same k-values where the poles of $S(k)$ are. One can see in Fig. 2 that the peaks form a single group of poles (mountain), but there are

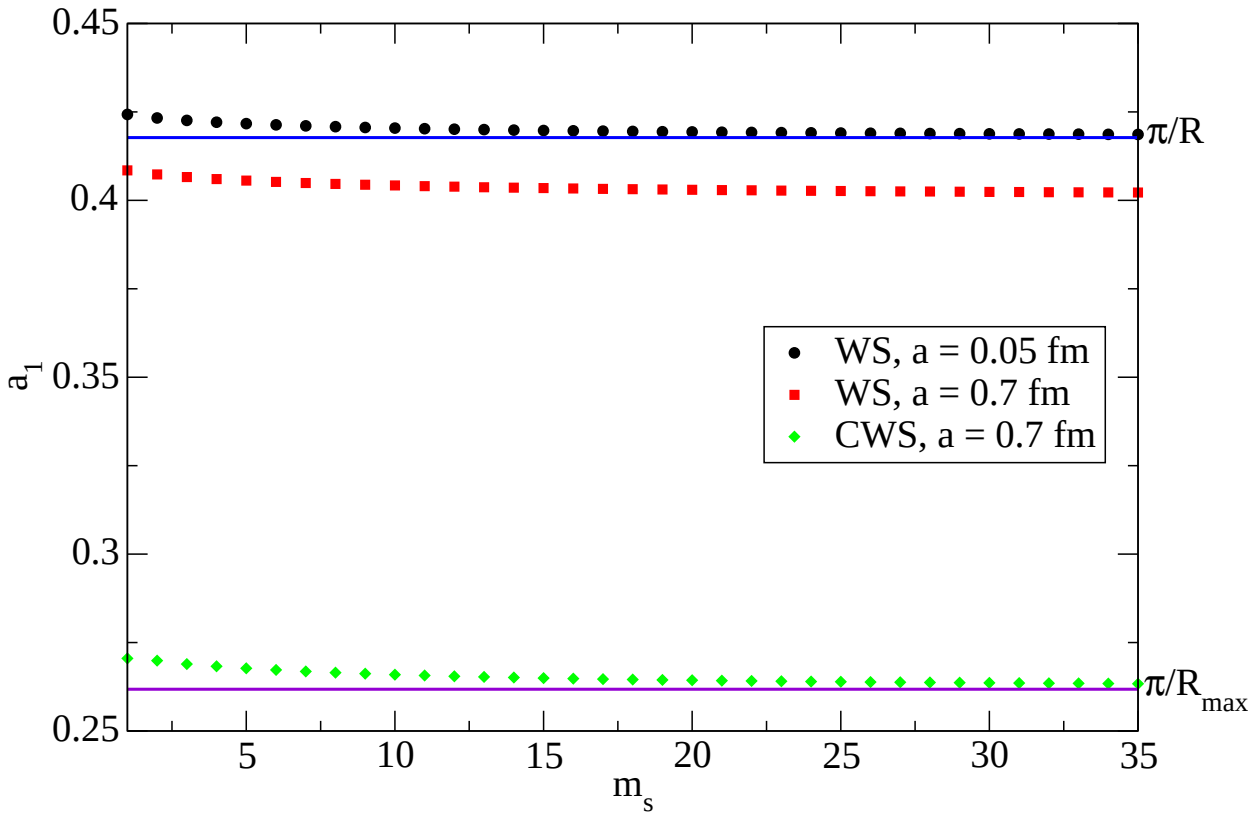

Figure 3: Dependence of the slopes of the fitted lines on the lower cut value of the sequence number of the pole m_s for the WS and CWS potentials, for $l = 0$ and with parameters: $V_1 = 44.4$ MeV, $R = 7.52$ fm $a = 0.7$ fm (red squares), $a = 0.05$ fm (black circles). $R_{max} = 12$ fm for CWS potential (green diamonds). The first order polynomials were fitted to the $|k_m|$ values. The horizontal lines correspond to the values π/R (blue line) and π/R_{max} (violet line).

more peaks for CWS potential than in Fig. 1 for the WS potential.

It is interesting to study how the pole positions change as the diffuseness parameter a of the CWS potential approaches zero to simulate a SQ potential.

As the value of the diffuseness is reduced another mountain starts to develop at low k^R values. A similar phenomenon can be observed in the case of ^{56}Fe in Fig. 6. The other mountain joins to the first mountain as m increases (at higher energy). Reducing the diffuseness further the second mountain moves away from the first one.

It was observed in Ref. [15] that close lying resonances interact with each other, therefore we analyze the first mountain only when the other one is far enough not to interact with the resonances of the first mountain.

For a smoother CWS potential with $a = 0.7$ fm the reflection at R is negligible and the radial wave function is reflected only at R_{max}. Poles of the CWS in this case form a single mountain with slopes close to the value of π/R_{max}, see Fig. 3. The R_{max} dependence of the slope of the fitted first order polynomial are shown in Fig. 4. This dependence on the unphysical parameter R_{max} is an inconvenient feature of the CWS potential [21].

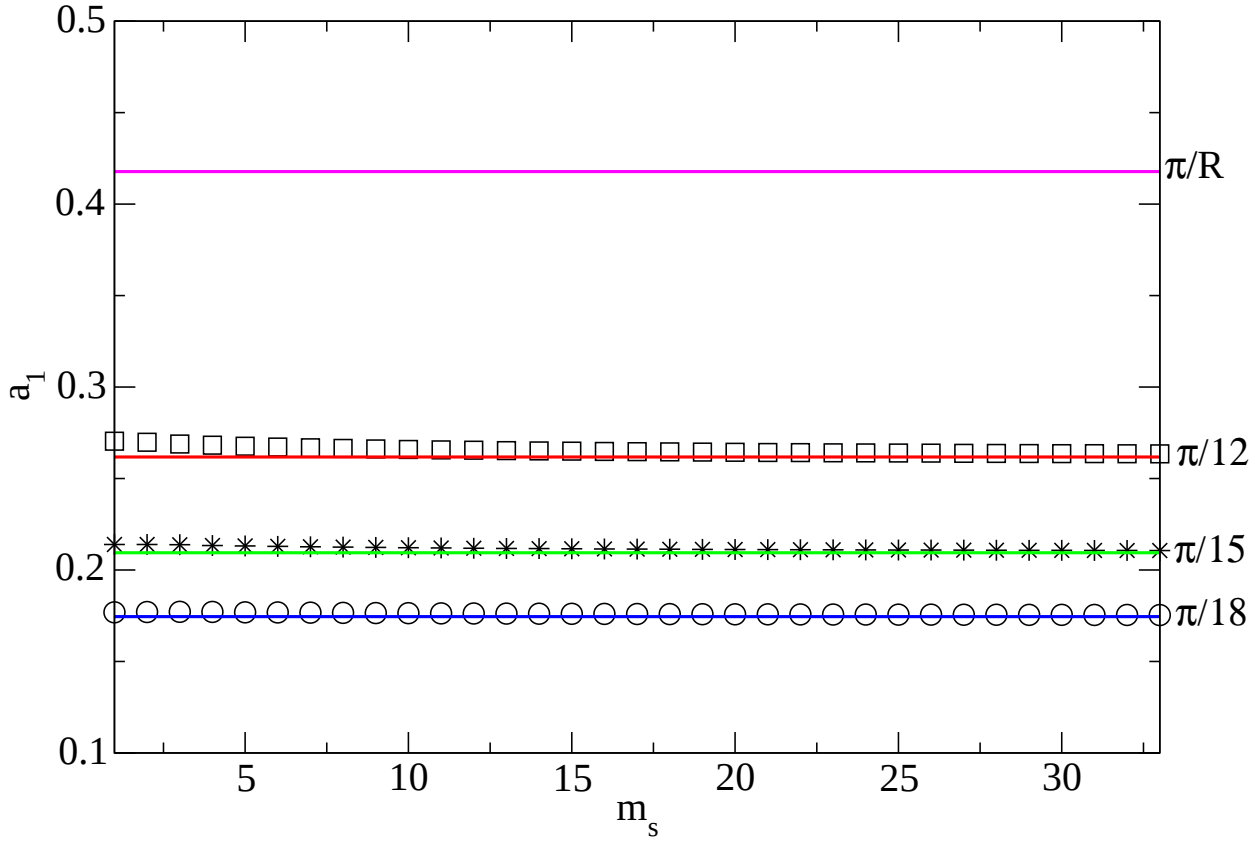

Figure 4: Dependence of the slopes of the fitted lines on the lower cut value of the sequence number of the pole m_s for the CWS potentials, for $l = 0$ and with parameters: $V_1 = 44.4$ MeV, $R = 7.52$ fm $a = 0.7$ fm for different R_{max} values. Squares for $R_{max} = 12$, stars for $R_{max} = 15$, circles for $R_{max} = 18$. The first order polynomials were fitted to the $|k_m|$ values. The horizontal lines corresponds to the values π/R (magenta) and π/R_{max}, with $R_{max} = 12$ (red line), $R_{max} = 15$ (green line), $R_{max} = 18$ (blue line).

6.3. CWS and CGWS potentials for a lighter system

The lighter system is the ^{56}Fe+n system studied by Bayrak and Aciksoz [7]. They used GWS and CGWS potentials for calculating bound state energies in that system and found reasonable good agreements between the bound state energies calculated by the analytical method and the numerical one with cut-off potential. Now we extend the studies for resonant states and want to investigate the effect of the cut-off on the positions of the resonant poles.

In Fig. 5 one can see the radial shapes of the CGWS potential with strengths $V_1 = 47.78$ MeV and $V_2 = -200$ MeV, $R = 4.92$ fm, $a = 0.6$ fm. The parameters were taken from Bayrak [7]. Here the dashed red curve is the dot-dashed curve in Fig. 1 of that paper. One can see in the figure that the surface term with negative V_2 strength produces a barrier in the GWS potential. The result of the barrier is the appearance of a few narrow resonances in that potential. If the barrier is high, then there are more narrow resonances. If we cut the tail of the GWS potential we introduce extra reflections at the cut-off radius beside the

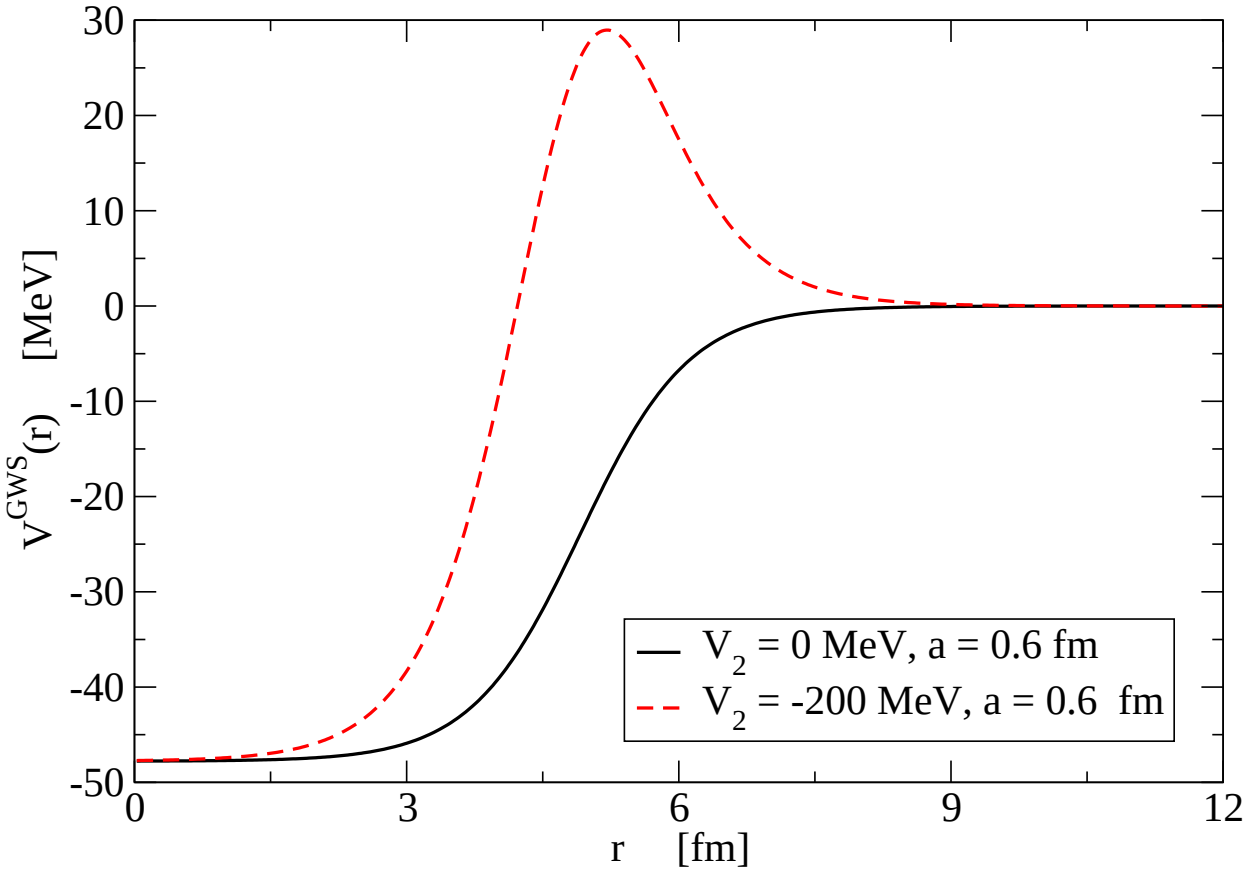

Figure 5: Radial shapes of the GWS potentials combined from attractive volume and repulsive surface terms with parameters: $V_1 = 47.78$ MeV and $V_2 = -200$ MeV, $R = 4.92$ fm, $a = 0.6$ fm.

ones at the nuclear radius R.

In Fig. 6 we plot the landscape of the function $-F(k)$ in the domain $k^R \in [-0.1, 5]$ fm^{-1}, $k^I \in [-1.2, 0]$ fm^{-1} calculated by using CGWS potential. The positions of the poles for GWS and CGWS potentials are shown in Fig. 7. Positions of the poles in GWS are denoted by black circles.

The poles of the GWS without cut are distributed quite regularly on the k-plane. If we fit the m-dependence of their $|k_m|$ values, the slope of the first order polynomial a_1 gives a range value $\mathcal{R}$ being very close to $R = 4.92$ fm. Therefore the reflection of the wave function happens at the radius of the GWS potential.

The poles for CGWS potential are denoted by red squares in Fig. 7. These poles were calculated by the program JOZSO. The results of the perturbation correction to the cut-off are denoted by green stars. Numerical values of the resonant pole positions are listed in Table 1.

The first line in Table 1 shows one pole in WS and CWS potential without barrier. There is no narrow resonance in this case. The resonance in the CWS potential was selected as the closest pole to that of the WS potential shown in the first row. The correction of k

Table 1: Dependence of the complex k_m wave numbers of the $l = 0$ poles of the S-matrix on the V_2 strength of the surface term for ^{56}Fe+n in the GWS potential. Analytical results were calculated by the code BENCZE, the numerical results were calculated by the program JOZSO [17]. The corrected k_m^{corr} values were calculated using Eq. (37). The cut-off radius value was $R_{max} = 12$ fm. The strength of the volume term were kept fixed at $V_1 = 47.78$ MeV. V_2 is given in MeV, and all wave numbers are in fm^{-1} units.

V_2	k_m^R(BENCZE)	k_m^I(BENCZE)	k_m^R(JOZSO)	k_m^I (JOZSO)	Re(k_m^{corr})	Im(k_m^{corr})
0	1.18982	−0.73207	1.15854	−0.61148	1.16310	−0.65090
−50	0.62716	−0.41298	0.62731	−0.41300	0.62716	−0.41297
−50	1.56608	−0.62284	1.57202	−0.62082	1.56615	−0.62244
−50	2.26765	−0.83134	2.43836	−0.75586	2.42596	−0.78478
−100	0.94090	−0.21067	0.94088	−0.21071	0.94090	−0.21067
−100	1.70535	−0.47048	1.70194	−0.46605	1.70482	−0.47034
−100	2.37343	−0.69445	2.40312	−0.63339	2.39838	−0.64374
−200	1.24873	−0.07323	1.24873	−0.07323	1.24873	−0.07323
−200	1.89306	−0.29392	1.89311	−0.29429	1.89306	−0.29392
−200	2.51849	−0.52297	2.53211	−0.49802	2.52623	−0.51614

brings the pole in the CWS potential somewhat closer to the one in the WS potential but the agreement is doubtful.

The surface term with $V_2 < 0$ produces a potential barrier. As the height of the barrier increases, the differences between the wave numbers calculated by the program BENCZE and that of program JOZSO, respectively become much smaller than the difference for $V_2 = 0$ in the first row of the table. The first and the second lines at each V_2 values show narrow resonances, where the CGWS results and their corrected values approach reasonably accurately the GWS results in the second and third columns of the table. The agreement for the third resonances is not so convincing therefore we suspect that the given form of the first order perturbation correction in Eq. (32) does not work so well for not narrow resonances. For the rest of the resonances not shown in the table, the differences of the k values in the potentials without cut and with cut-off are considerably larger. The correction term in Eq. (32) is clearly unable to correct the increasingly large differences originating from the cut-off the potential for broader resonances.

Three groups of poles can be observed in Fig. 7. The group A consists of the first three poles lying closest to the real axis. They are the narrow resonances listed in the last three rows and fourth and fifth columns of the Table 1. The positions of these narrow resonances approximate well the corresponding poles of the GWS potential calculated by the code Bencze. The results of the correction improve the agreement even further. The general behaviour of these group of resonances is similar to that of the resonances in GWS potential, namely that the distance of the resonances in group of A is determined by the radius R of the CGWS potential. They are caused by the reflection of the radial wave

function at the nuclear radius R. The A group of poles proceeds with another group (B) in which the distance of poles is much smaller and it is determined by the cut-off radius $R_{max} = 12$ fm. The poles in group B are due to the reflection of the wave function at the cut-off radius. The third group of poles (C) is composed of the five remaining broadest resonances in Fig. 7. We suspect that they are most probable due to the double reflections at R and R_{max}. Their distance is determined approximately by the difference $R_{max} - R$, as one can see in Table 2, where we varied the value of R_{max}. The largest difference is between $R_{max} - R$ and $\mathcal{R}$ is for $R_{max} = 21$ fm. We suspect that it is due to the combined effect of the accumulation of numerical errors during the largest distance and the interaction with the closest poles in the other groups.

Table 2: Comparism of the ranges calculated from the best fit first order polynomial in Eq. (18) for the group of resonances B, A, C of the ^{56}Fe+n system in the CGWS potential with parameters: $V_1 = 47.78$ MeV, $V_2 = -200$ MeV, $R = 4.92$ fm, $a = 0.6$ fm. Ranges $\mathcal{R}_A$, $\mathcal{R}_B$, $\mathcal{R}_C$ are the ranges corresponding to the groups A, B and C.

R_{max}	$\mathcal{R}_B$	R	$\mathcal{R}_A$	$R_{max} - R$	$\mathcal{R}_C$
15	14.9999	4.92	4.8356	10.08	10.1911
18	18.0360	4.92	4.7776	13.08	13.3406
21	21.0829	4.92	4.7864	16.08	17.4930

The perturbation corrections in Eq. (37) are not large enough for the poles in group B and C to bring these poles to the vicinity of the poles calculated by the code BENCZE. Therefore the correction works well only for the narrow resonances in group A.

The resonances in group A can be considered as physical resonances, since there positions depend on the physical parameters of the GWS potential and they are practically independent of the cut-off radius. The (in)dependence of the positions is shown in Table 3. The position of the $m = 1$ resonance does not change when the value of the R_{max} increased to 21 fm from 12 fm. A similar increase of the R_{max} value changed the positions of k_2 and k_3 only in the last three decimal digits. So the dependence on the unphysical parameter can be neglected for this group of resonances.

In Fig. 7 the positions of the first three resonances in group A are on the top of the resonances of the GWS potential. The differences are small and can not be seen on the scale of the figure. The corrected eigenvalues of these three resonances are on the top of the resonances of the GWS potential, because the corrections are also small for these narrow resonances.

For the resonances in group A the pole position is practically independent of the cut-off radius (Table 3), and the results of the programs BENCZE and JOZSO are almost the same, as one can see in Table 1. The number of the narrow resonances increases with the height of the barrier.

Fig. 8 shows the normalized radial wave function for one of the narrow resonances in CGWS potential with parameters: $V_1 = 47.78$ MeV and $V_2 = -200$ MeV, $R = 4.92$ fm, $a = 0.6$ fm and $R_{max} = 12$ fm. It is the $m = 2$ resonance in Table 3 . In the figure the real

Table 3: Dependence of the complex k_m wave numbers of the $l = 0$ poles of the S-matrix on the value of R_{max} for the three narrow resonances of the ^{56}Fe+n system in the CGWS potential with parameters: $V_1 = 47.78$ MeV, $V_2 = -200$ MeV, $R = 4.92$ fm, $a = 0.6$ fm.

m	R_{max}	k_m^R	k_m^I
1	15.0	1.24873	−0.07323
1	18.0	1.24873	−0.07323
1	21.0	1.24873	−0.07323
2	15.0	1.89305	−0.29393
2	18.0	1.89306	−0.29392
2	21.0	1.89306	−0.29392
3	15.0	2.51152	−0.52311
3	18.0	2.51952	−0.52337
3	21.0	2.51840	−0.52283

and the imaginary parts of the resonant wave function oscillate around the zero axis. In the external region ($r > R$) the magnitudes of the oscillations increase as r increases. In the internal region of the potential, the number of zeros of the real part of the wave function is 3. If we make a similar plot for the $m = 1$ resonant wave function the number of zeros of the real part of the wave function is 2. This is in agreement with the finding in Ref. [7] in which the 0s and 1s states of the ^{56}Fe are bound states.

For narrow resonances the number of zeros of the real parts can be considered as the generalizations of the node number n of the bound states. The imaginary part of the wave function also oscillates around the zero axis with exponentially growing amplitudes in the external region. Here the phase of the oscillations is shifted wrt that of the real part. For this narrow resonance the magnitude of the internal oscillations is smaller than that of the real part, and the crossing points of the zero axis are not far from the crossing points of the real part. We observed that these features are general characteristics of the Gamow wave functions for narrow resonances. In certain respect the narrow resonances resemble to the bound states and they are sometimes called as *quasi-stationary states*. For the quasi-stationary states the corrections due to the cut-off the tail of the potential are small and their k eigenvalues are not very sensitive to the cut-off distance as we demonstrated it in Table 3.

As the imaginary parts of k become larger, the tail region moves inward, the imaginary part of the wave function competes with the real part. At the same time the value of the cut-off distance becomes more important and the k pole position of the CGWS potential moves away from the k of the GWS potential, as one can see in Fig. 7. The strong dependence on the cut-off distance was noticed earlier by two of us in Ref. [22] for resonances with $l = 5$.

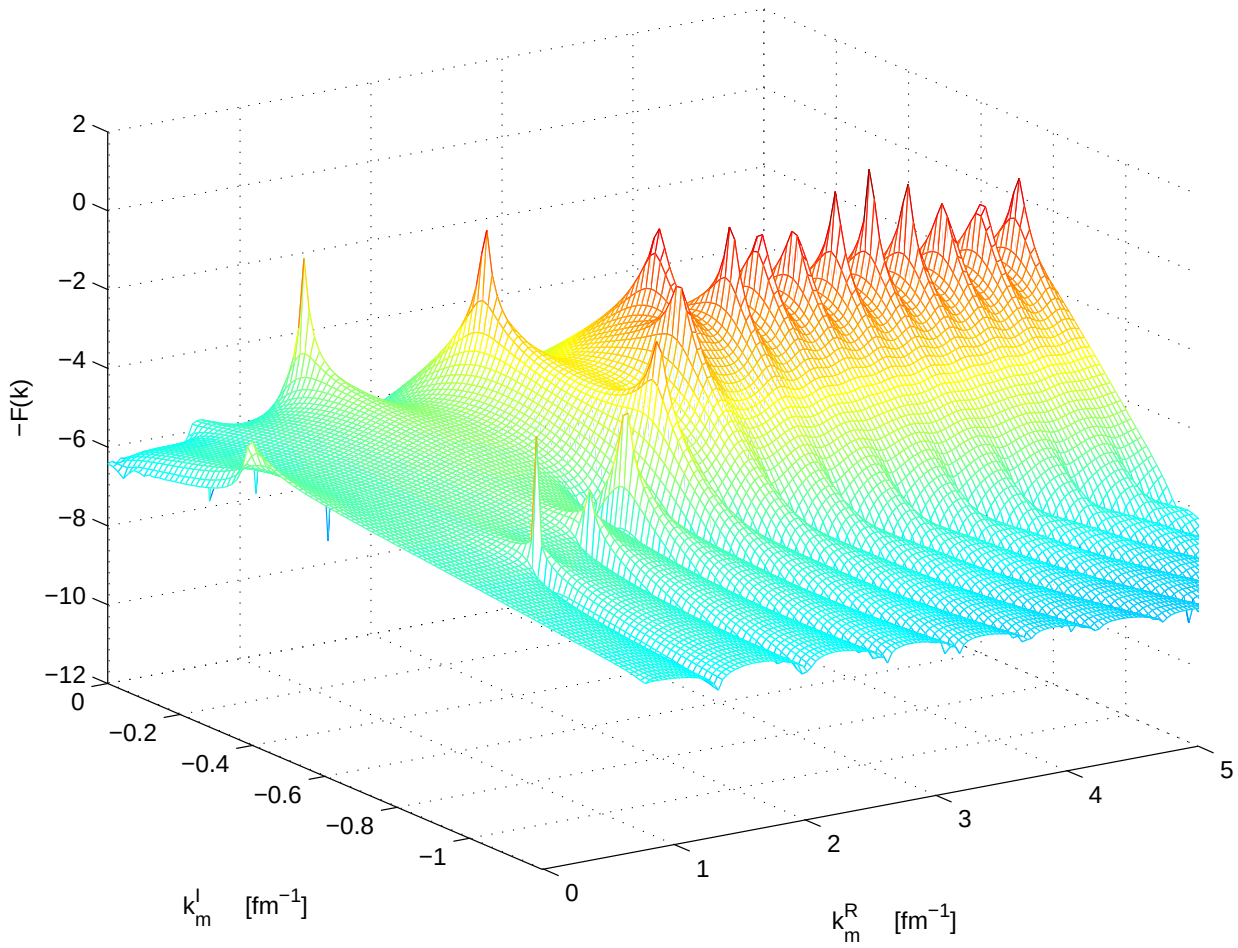

Figure 6: $-F(k)$ on the domain $k^R \in [-0.1, 5]$ fm^{-1} and $k^I \in [-1.2, 0.0]$ fm^{-1} calculated for a CWS potential with depth parameter: $V_1 = 47.78$ MeV, $V_2 = -200$ MeV, $a = 0.6$ fm, $R = 4.92$ fm, $R_{max} = 12$ fm for ^{56}Fe +n system.

7. Summary

We have investigated the effect of the cutting the tails of the WS and GWS potentials for the resonant poles of the S-matrix by calculating the pole positions. For zero angular momentum the radial Schroedinger equation is solved by using the analytical formula of Gy. Bencze [1]. The positions of the poles were calculated with high precision by the program BENCZE written in Wolfram Mathematica. The cut-off versions of the same potentials, the CWS and CGWS potentials were studied by solving the radial equation numerically by the FORTRAN program JOZSO [17]. Pole distributions were studied by exploring the landscape of the modulus of the complex function $-F(k)$, which has maxima at the same k positions as the $S(k)$-matrix. The maxima of the function supplied us with starting values for finding the accurate positions of the poles. Presenting the landscapes of the $|S(k)|$ and the $|-F(k)|$ functions gives an excellent tool to demonstrate the differences of the pole distributions of the potentials without cut and with cut at finite distance. With the absence

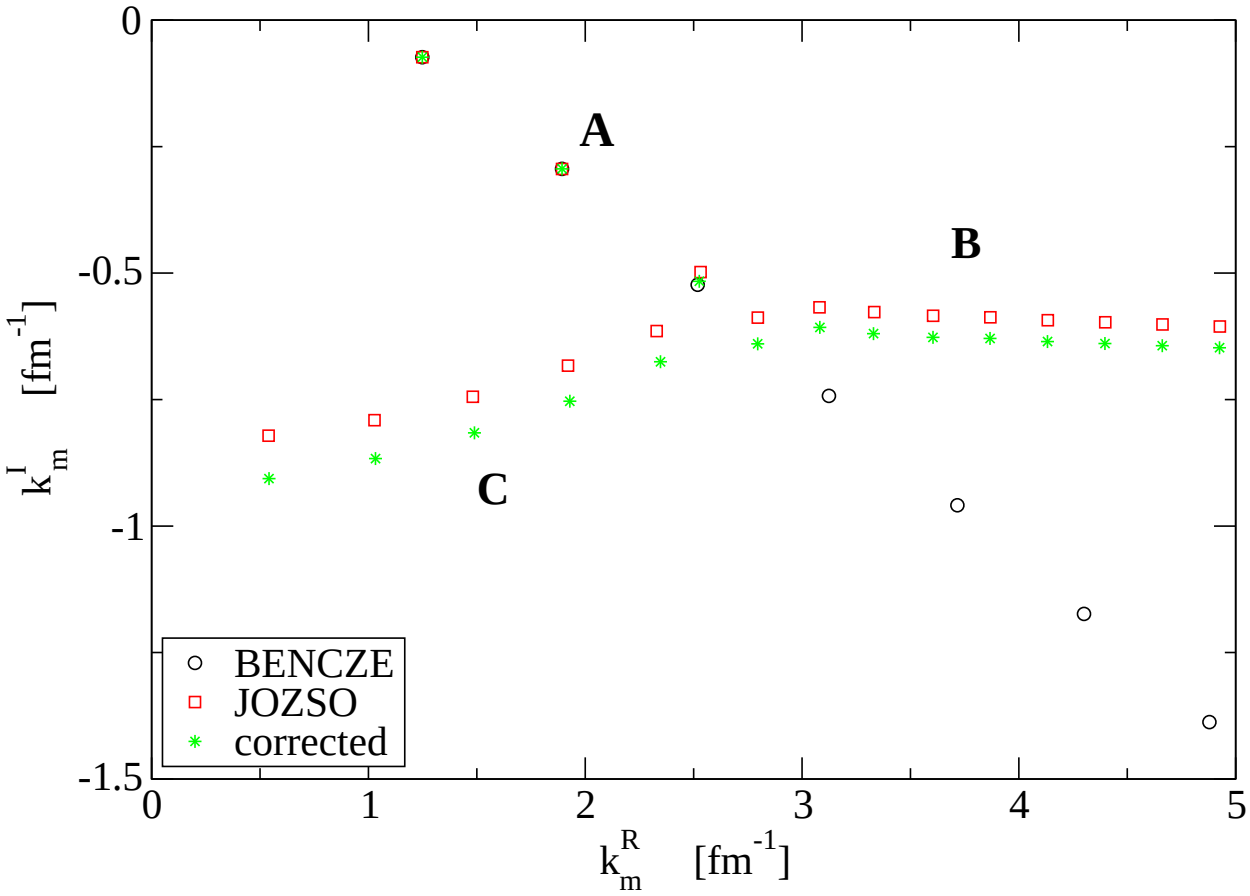

Figure 7: Positions of the poles in GWS and in CGWS potentials with parameters $V_1 = 47.78$ MeV and $V_2 = -200$ MeV, $R = 4.92$ fm, $a = 0.6$ fm and $R_{max} = 12$ fm without and with correction.

of the surface term of the GWS potential we can study the normal WS and CWS potentials and the effect of the cut of their tails.

The pole structure of the WS and the CWS potential is basically different as it was pointed out by R. Newton [10]. The WS and the GWS potentials produce one group of poles (mountain) similar to that of the square well potential with the same nuclear radius. From the slopes of the first order polynomials fitted best to the moduli of the k eigenvalues a range $\mathcal{R}$ can be deduced being very close to the nuclear radius parameter R. For these potentials the reflection of the radial wave function takes place at R.

The CWS and the CGWS potentials produce two or three groups of poles (mountains). They are more visible if in the CGWS potential a repulsive surface term is present and we have a potential barrier producing a few narrow resonances. The positions of the narrow resonances are similar to those of the GWS potential, they form a first group of poles in which the distance of the poles are similar to that of the square well potential with radius R.

The appearance of the second and sometimes the third group of poles is apparently due to the cut of the CWS potential. The poles in the two different mountains are labelled

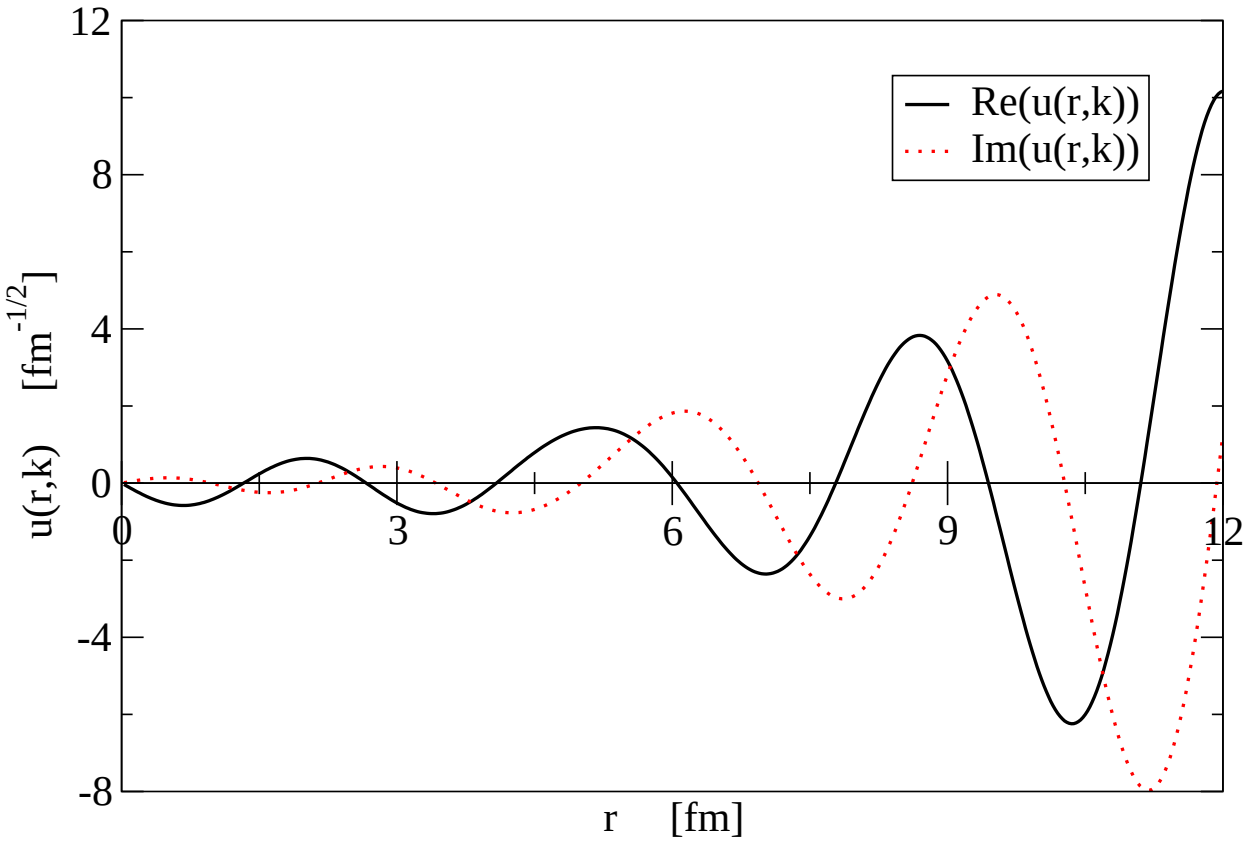

Figure 8: Radial shapes of the $m = 2$ normalized resonant wave function with $k = (1.893, -0.294)$ fm^{-1} in CGWS potential with parameters: $V_1 = 47.78$ MeV and $V_2 = -200$ MeV, $R = 4.92$ fm, $a = 0.6$ fm, $R_{max} = 12$ fm.

separately by indexing the order of their k^R values. The moduli of the $|k_m|$ values in both mountains can be approximated by first order polynomials as the function of the m values. From the a_1 slopes of these polynomials one can derive a sort of distance where reflection of the solution takes place. We assume that the appearance of the poles for broad resonances is due to reflections at these distances. Reflections take place when the derivative of the potential has sudden change. In a square well this evidently happen at its radius R. For GWS potentials for small values of the diffuseness the derivatives are still large and the wave functions are reflected at the nuclear radius R. For a CGWS potential the potential has a jump at the cut-off radius R_{max} where the derivative does not exist. This causes a reflection of the wave function at this distance, and the distance of the poles in the first mountain of the diffuse well is influenced by this reflection. The $\mathcal{R}$ distances calculated from the slope of the best fit linear polynomials therefore are very close to the value of R_{max}.

For small diffuseness and for not very large energy the radial wave function can be reflected at R and at R_{max} as well and oscillations between these two distances produces the third group of poles (mountain).

The effect of cutting off the tail of the potential is too large for the second and the third

group of poles and the first order perturbation correction is unable to recover the cut.

The numerical results were performed for two different nuclear systems, the heavy target case for ^{208}Pb+n system and for a lighter system for ^{56}Fe+n system studied recently by Bayrak and Aciksoz [7]. We observed similar results for the light and the heavy target systems, as far as the reflections of the wave function are concerned and conclude that our results are typical for the nuclear potentials studied.

Acknowledgement

Authors are grateful to L. Gr. Ixaru and A. T. Kruppa for valuable discussions. This work was supported by the Hungarian Scientific Research – OTKA Fund No. K112962.

References

[1] Gy. Bencze, Commentationes Physico-Mathematicae **31**, 4 (1966).
[2] G. Lévai, Int. J. Theor. Phys. (2015) **54**, 2724.
[3] R. D. Woods, D. S. Saxon, Phys. Rev. **95**, 577 (1954).
[4] N. Michel, W. Nazarewicz, M. Płoszajczak, and T. Vertse, J. Phys. G. **36**, 013101 (2009).
[5] K. Fossez, N. Michel, M. Płoszajczak, Y. Jaganathen, and R. M. Id Betan, Phys. Rev. C **91**, 034609 (2015).
[6] P. R. Kumar, and B. R. Wong, AIP Conference Proceedings **1657**, 160001 (2015).
[7] O. Bayrak and E. Aciksoz, Phys. Scr. **90**, 015302 (2015).
[8] M. Abramowitz and I A. Stegun, Handbook of Mathematical Functions, Dover Publ. Inc., New York 1965.
[9] H. M. Nussenzveig, Nucl. Phys. **11**, 499 (1959).
[10] R. G. Newton, Scattering Theory of Waves and Particles, Springer Verl., New York Inc., 1982.
[11] J. Darai, A. Rácz, P. Salamon, and R. G. Lovas, Phys. Rev. C **86**, 014314 (2012).
[12] P. Salamon, R. G. Lovas, R. M. Id Betan, T. Vertse, and L. Balkay, Phys. Rev. C **89**, 054609 (2014).
[13] T. Vertse, K. F. Pál, Z. Balogh, Comput. Phys. Commun. **27**, 309 (1982).
[14] L. Gr. Ixaru, M. Rizea, T. Vertse, Comput. Phys. Commun. **85**, 217(1995).
[15] Á. Baran, Cs. Noszály, P. Salamon and T. Vertse, European Physical Journal A, **51**: 76 (2015).
[16] L. Gr. Ixaru, Numerical Methods for Differential Equations, D. Reidel, Publ. Comp., Dordrecht/Boston/Lancaster, 1984.
[17] Cs. Noszály, Á. Baran, P. Salamon, and T. Vertse, *JOZSO, a renewed version of the computer code GAMOW for calculating broad neutron resonances in phenomenological nuclear potentials*, to be submitted to Computer Physics Communications.
[18] W. H. Press, B. P. Flannery, S. A. Teukolsky, W. T. Vetterling, Numerical Recipes, Cambridge University Press, Cambridge, 1987.
[19] T. Berggren, Nucl. Phys. **A109**, 265 (1968).
[20] T. Vertse, P. Curutchet, and R. J. Liotta, Lecture Notes in Physics, 325, pp 179-200. Proceedings, Lertorpet, Sweden, 1987.
[21] A. Rácz, P. Salamon, and T. Vertse, Phys. Rev. C **84**, 037602 (2011).; P. Salamon, and T. Vertse, Phys. Rev. C **77**, 037302 (2008).
[22] P. Salamon, and T. Vertse, Phys. Rev. C **77**, 037302 (2008).